# The V-SHARK high contrast imager at LBT

Pedichini, F., Ambrosino, F., Centrone, M., Farinato, J., Li Causi, G., et al.

# "The V-SHARK high contrast imager at LBT."

F. Pedichini*[a], F. Ambrosino [a], M. Centrone [a], J. Farinato [b], G. Li Causi [a], E. Pinna [c], A. Puglisi [c], M. Stangalini [a], V. Testa [a] and the SHARK science Team[**]

[a]INAF OAR, Via Frascati 33, 00087 Monteporzio Catone (RM) Italy; [b]INAF OAPD, Vicolo Osservatorio 33 Padova Italy; [c]INAF Arcetri, Firenze Italy.

## ABSTRACT

In the framework of the SHARK project the visible channel is a novel instrument synergic to the NIR channel and exploiting the performances of the LBT XAO at visible wavelengths. The status of the project is presented together with the design study of this innovative instrument optimized for high contrast imaging by means of high frame rate. Its expected results will be presented comparing the simulations with the real data of the "Forerunner" experiment taken at 630nm.

**Keywords:** High angular resolution, Imaging, Adaptive Optics, Exoplanets

## 1. INTRODUCTION

The V-SHARK main goal is to open new observational frontiers at LBT on narrow fields, *allowing diffraction limited* high contrast imaging in the visible (from 600 to 900 nm). This will be obtained taking advantage of the high performance of the XAO system already installed on the telescope [1].

Indeed the LBT telescope diffraction limit ($\lambda$/D @ 650nm) is around 16 mas, and allows to resolve very close star systems and to detect companions with a contrast as high as $\approx$ 14mags separated by only 100 - 150mas (after data reduction with ADI or similar techniques). This contrast in detection may also be improved by a factor 2 or 3 ($\approx$ 1mag) using the planned V-SHARK coronagraphic modality. The instrument design integrates the facilities to deploy aperture masks at the telescope focal plane and GRISMs or polarizers in the pupil plane, to allow low dispersion field spectroscopy and polarimetry. Furthermore V-SHARK is designed to record small field (1.5" x 1.5") images at 1kHz cadence to exploit Lucky imaging, freeze the atmosphere turbulence for AO speckle imaging or applying deconvolution from wavefront sensor data methods [2]. The typical sources, were to operate V-SHARK, have magnitude R < 13, nevertheless it may be also a very sensitive imager due to the low noise of its sCMOS detector.

Thanks to the LBTI-XAO and its future upgrade [3], V-SHARK can reach the magR $\approx$ 26 in a few minutes of integration, when operated 5" off-axis from a bright guide star with Strehl ratios of the order of 30%. In binocular operations, it will be complementary to NIR-SHARK [5], extending its wavelength coverage (from 600 to 2000 nm) in the visible bands, simultaneously.

The V-SHARK technical description, its expected science results and the management needed to deploy this new project in a *fast track* timeline of 2 years at LBT are described in the following parts of this paper.

### 1.1  V-SHARK Project History

In 2012, the LBT First Light Adaptive Optics (FLAO) demonstrated its unique capabilities [1], delivering excellent results in terms of performance and reliability. Motivated by that, we started out investigating the technical feasibility, and the scientific impact, of a camera for direct imaging and coronagraphy to be implemented at LBT. Due to the large wavelength range that SHARK (System for coronagraphy with High order Adaptive optics from R to K band) would explore, several possible instrument layouts were presented, finally converging to a binocular approach with two separated channels.

The SHARK project at LBT was then presented, on February 2014 in the framework of the *"2014 Call for Proposals for Instrument Upgrades and New Instruments"*, with two channels, each one of them installed on a different telescope arm, namely the Visible channel (hereafter V-SHARK [6]) and the Near Infra-Red channel (NIR-SHARK [7]). Both channels will be equipped, with at least one camera providing direct and coronagraphic imaging.

SHARK is planned for the LBT 2nd generation instrumentation but, in the proposed configuration, it is designed to co-exist with the currently available instrumentation, being placed at the entrance of LBTI and sharing part of the wavelength domain with it on both its channels (Figure 1).
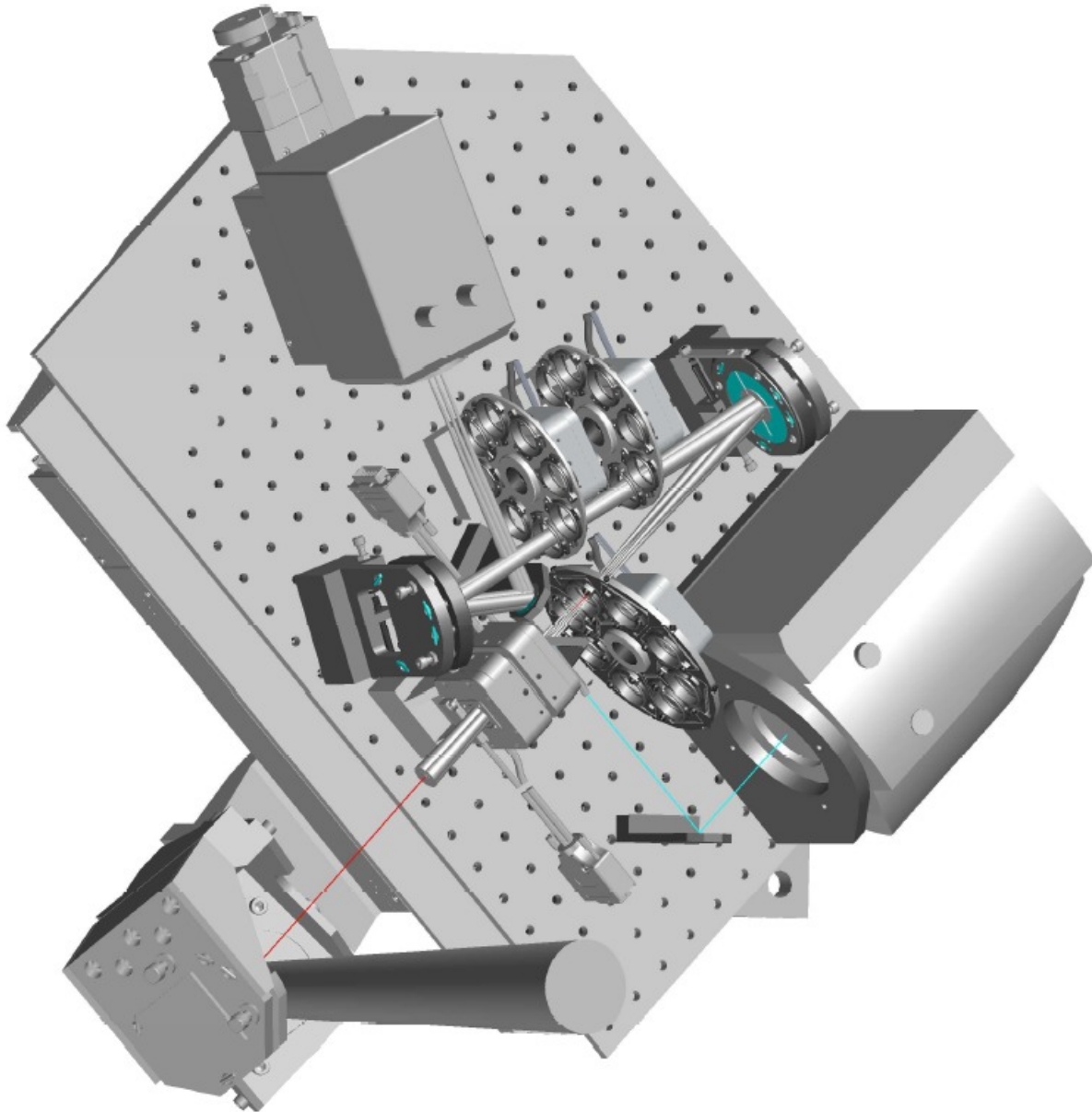


Figure 1: V-SHARK CAD render of the baseline instrument. The dust cover is here removed to show internal opto-mechanic components.

## 2. V-SHARK SYSTEM DESCRIPTION

### 2.1 V-SHARK Guidelines

The basic ideas behind V-SHARK architecture are *minimalism and fast track*. Of primary importance for the project plan and architecture it is to exploit the already existing WFS, instead of deploying a new WFS module specifically designed

for the purposes of this instrument. This means that, the overall SHARK project must be designed to be compliant with existing WFS and FLAO mode, and to exploit them the most. The *V-SHARK Forerunner experiment* [4] positively assessed on sky the effectiveness of this concept on 2015.

For a better understanding of the V-SHARK system architecture, it is important at first, to consider it as an instrument downstream of the powerful LBT-XAO system whose typical performances on bright sources are summarized in Figure 2 where the expected PSF Strehl ratio is plotted *vs* wavelength.
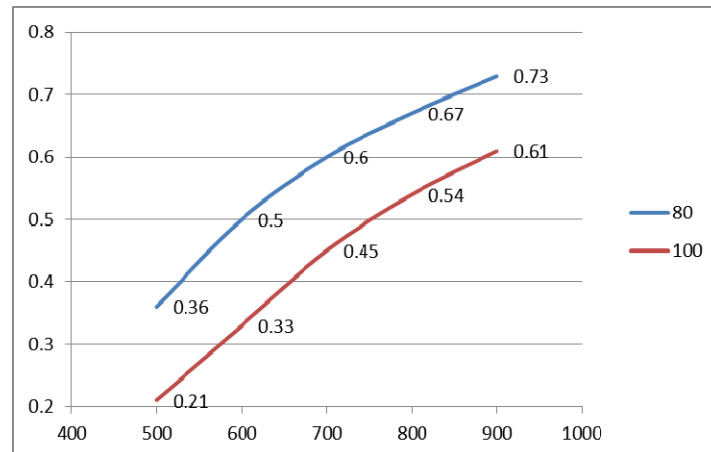


Figure 2: Estimated Strehl ratio (according to the Marechal law) as a function of the V-SHARK wavelength range for the 80 and 100 nm typical LBTI-AO residual rms wavefront error on bright sources with 0.6 – 0.8 arcesc seeing.

## 2.2 System architecture description

V-SHARK is conceived to allow an easy replacement of parts and simple upgrades from its baseline. It will share as much as possible opto-mechanic components with NIR-SHARK and will use COTS (Components Off The Shelf). Big or heavy moving parts are only limited to the deployable light beam pick-up and the camera focus. V-SHARK system level architecture is assembled with a few functional blocks presented in Figure 3 together with a cad render of the assembled instrument. Following the successful experience of the Forerunner a robust steel optical breadboard is the common mechanical interface connecting all the functional blocks. This makes it easier their positioning and registering. This board is connected to the LBTI frame through a rigid metal interface shown in Figure 4. With reference to the right panel of Figure 3, following the light path the first part of V-SHARK is the Deployable Pick-Up. This has the function of holding the dichroic feeding the LBTI WFS and to mount a piezo tip-tilt mirror for the fine stabilization of the light beam through the ADC. The beam is then going to the f#15 focus where it is possible to place occulting masks. Before the f#15 focus a dichroic relays an image of the focal plane on a fast and sensitive EM-CCD guide camera, controlling the tip-tilt mirror, for an adaptive stabilization of the PSF jitter. This architecture allows also a sharp pointing of the PSF on coronagraph masks. A successive f#15 off axis parabola collimates the beam yielding a pupil plane of ∅10mm to place field stops and filters. Finally another off axis f#22 parabola slows the beam to achieve the desired sampling on the detector without the needs of further optical components. Enough space is provided between the V-SHARK sections to allow the deployment of multi-slot wheels and to position an IFU for a future fiber fed spectrograph. The detector focus is actuated by using an electrically controlled linear stage.
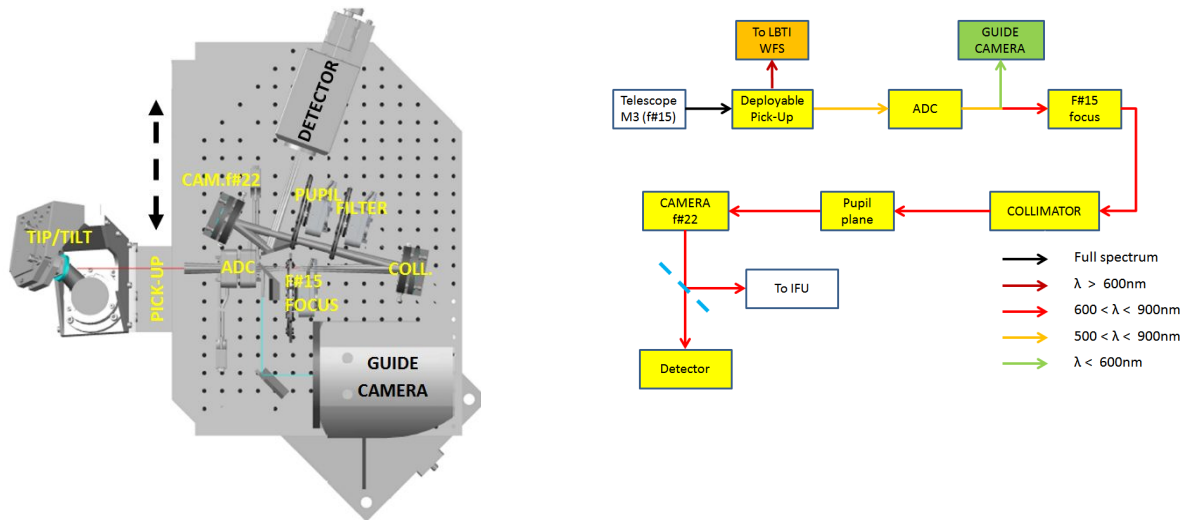
Figure 3. Left: Cad view of the assembly for reference with the system diagram. Right: system level description of V-SHARK architecture with its main functional blocks and light paths. Science path is in red. White modules are not considered parts of V-SHARK.
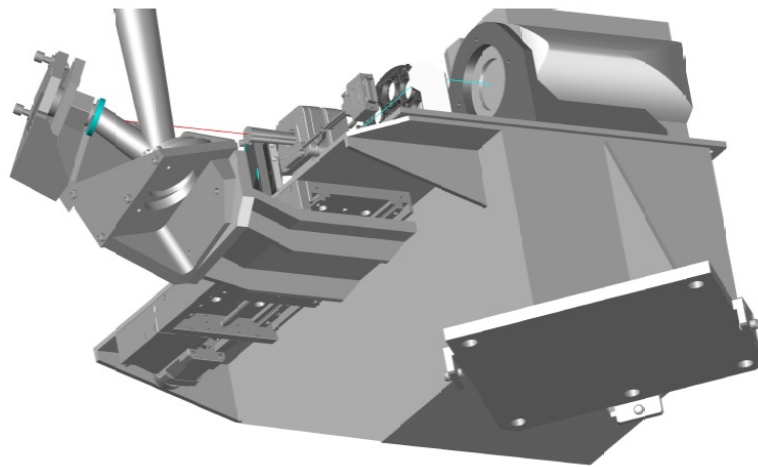


Figure 4: The mechanical interface of V-SHARK to the LBTI frame.

## 2.3 Location at LBT

The location of V-SHARK close to the right LBTI [9] input window (see Figure 5), has been experimentally verified during the Forerunner experiment in 2014 and 2015. This location allows to position the V-SHARK close enough to the LBTI-AO WFS, in order to mitigate the effects of NCPA induced aberrations. The Forerunner experiment proved this approach, demonstrating a residual NCPA below 15nm that can be accounted by offsetting a few modes of the AO reconstructor.

Figure 5: The proposed mount location for V-SHARK in BLUE on the LBTI frame.

## 2.4  Optical Design

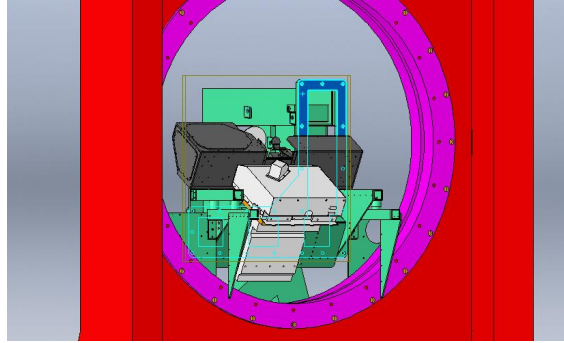The design of the V-SAHRK optics is based on the classical scheme of Richardson and follows the suggestion of Ghedina and Ragazzoni [8]. It is depicted in the following Figure 6 where the principal subsection are labelled. The final performances expected from this design (comprehensive of the ADC section) at 45 deg of Zenith distance are summarized in Figure 7.
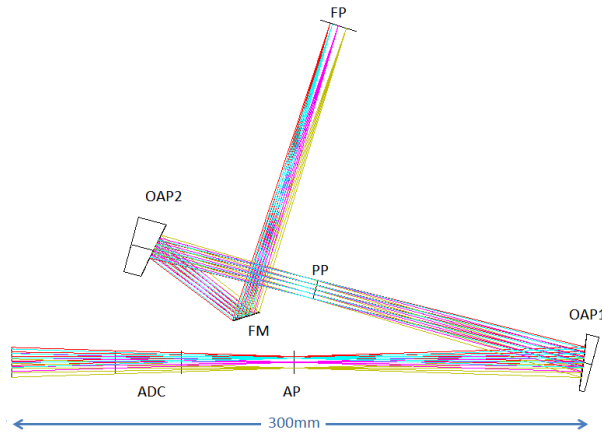


Figure 6: V-SHARK optics layout with labeled its main subsections.

The final V-SHARK optical performances are within the limits imposed by  the requirements of the TLRs, furthermore, in most of its observations the instrument will operate on a reduced field of view (typical <2"), with a limited spectral bandwidth where the performances will be also better. The project team selected a final focal plane sampling of 7.5 mas/pixel with the diameter of the FOV to be around 10", this allows the Nyquist sampling of the PSF up to 600nm.



Figure 7; Left: spot diagram, Center: encircled energy, Right: Strehl map of the proposed V-SHARK optical design at 45° of Zenith angle after ADC correction of the atmospheric dispersion on the full wavelenght range from 600 to 900 nm.

The minimal optical design guarantee a final optical throughput of about 29% (with atmosphere and telescope), while the only V-SHARK optics throughput is about 83% (detector excluded).
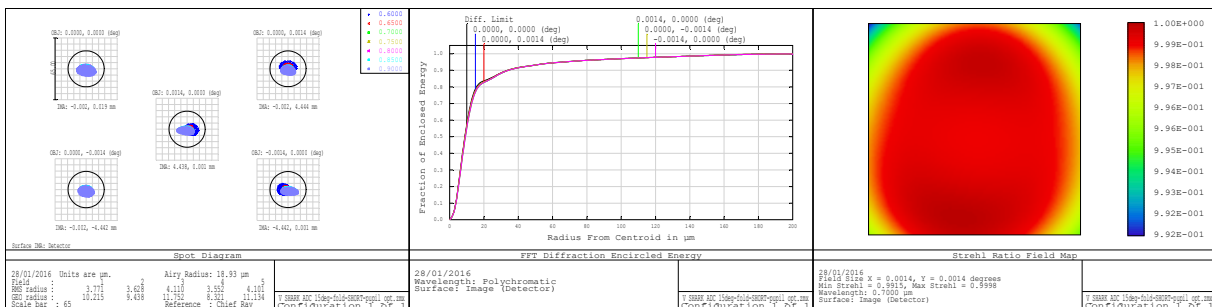
## 2.5 Detectors

There are two cameras in V-SHARK with different purposes:
- The imager to acquire science data
- The guider to provide feedback to the psf jitter stabilization system

The selected detector for the imager of V-SHARK is the Andor Zyla 4.2+ sCMOS while the EM-CCD technology of the Andor "iXon Ultra 897" is preferred for the V-SHARK guide camera. The following Table 1 summarize the main characteristics of this imagers. For further references please visit http://www.andor.com

Table 1: V-SHARK detector comparison table

| CAMERA MODEL | ANDOR Zyla 4.2+ | ANDOR iXon Ultra 897 |
|---|---|---|
| Function | imager | fast guider |
| Pixel # | 2k x 2k | 256 x 256 |
| Pixel size [μm] | 6.5 x 6.5 | 16 x 16 |
| RON [e$^-$] | ≈1 | <0.1 |
| Dark [e$^-$/s] | <0.02 | <0.01 |
| Frame rate [Hz] | 100 - 1000 | 50 - 5000 |
| QE [%] | 70 | 90 |
| Data Interface | USB 3.0 | USB 2.0 |

## 2.6 Controls

All the controls in V-SHARK will be interfaced to the high level control software following the LBTO specifications. In V-SHARK there are several devices to be controlled with a few microns precision and repeatability (see Figure 8). To simplify the overall control architectures we propose to standardize the axes driver to a common software platform (LabView or C/C++) interfaced to the USB bus of the V-SHARK computer as already shown in Figure 8. The rotary solution is preferred for the optical devices like masks and filters that can be housed in a multi-slot wheel moved with a brushless or a piezo step motor. Instead the tip/tilt control with its guide camera is managed by a dedicated μPC that communicates with the control PC via Ethernet line.

The two Andor imagers (Zyla4.2+ and iXon Ultra 897) have USB interfaces for control and images download. Both devices provide LabView, and C/C++ Win and Linux driver for interfacing in the V-SHARK control system both for engineering and high level control.
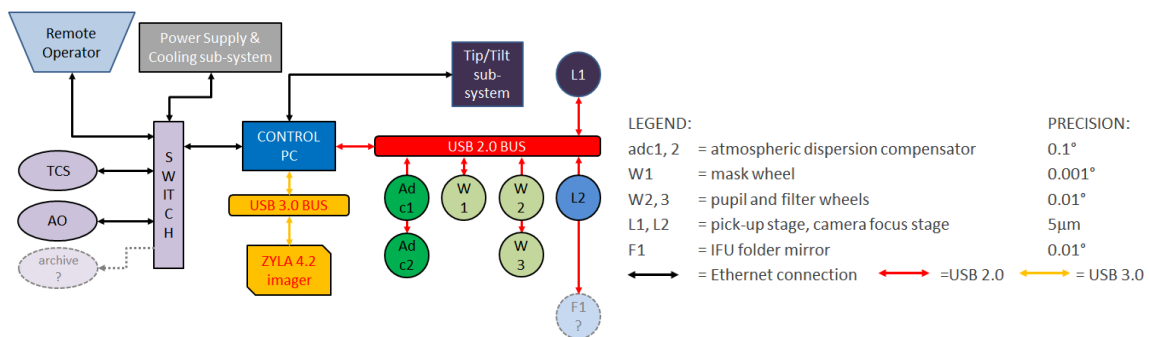


Figure 8: V-SHARK control architecture. Precision requested to the hardware devices are on the right side of the legend.

## 3.  EXPECTED PERFORMANCES ON SKY

A specific end-to-end SHARK simulation code (SSC) was developed on top of the extensively-tested IDL-PROPER library [12]. This library allowed us to model the optical propagation along the V-SHARK optical components, from the telescope aperture down to the focal plane, and to easily test different configurations for the hardware parameters like, for example, the diameter of the Lyot stop and the diameter of the occulting mask. In order to take into account the effects of the residual aberrations of the AO system, the SSC was designed to take into account the AO residual wave front distortions obtained from the realistic FLAO simulation code, and to propagate them along the optical path. In this way, the impact of different seeing conditions and AO configurations on the performances of the instrument can be easily evaluated and analyzed.

In this section we analyze 60 seconds exposures of a magnitude 8 star in R band at different seeing with almost steady seeing conditions and supposing a perfect subtraction of the instrument PSF.

Several fake sources were injected into the simulated data using a flux rescaled off-axis PSF. The coronagraph mask is either a solid Lyot disk or a Gauss transmission mask with different sizes. In the case of a Gauss mask, we recall that the radius is defined as the HWHM of the mask itself. The pupil mask has a 99.9% of its nominal diameter, with an internal occultation of 35%. This is done in order to remove secondary mirror diffracted light. With the aim of assessing the role of the background noise, photon noise and detector RON [1 e-/s] were added to the simulated images, avoiding the saturation of each image that composes the final long-exposure PSF. Noise level is assumed as the standard deviation of the collected photon number on a pixel-by-pixel basis.
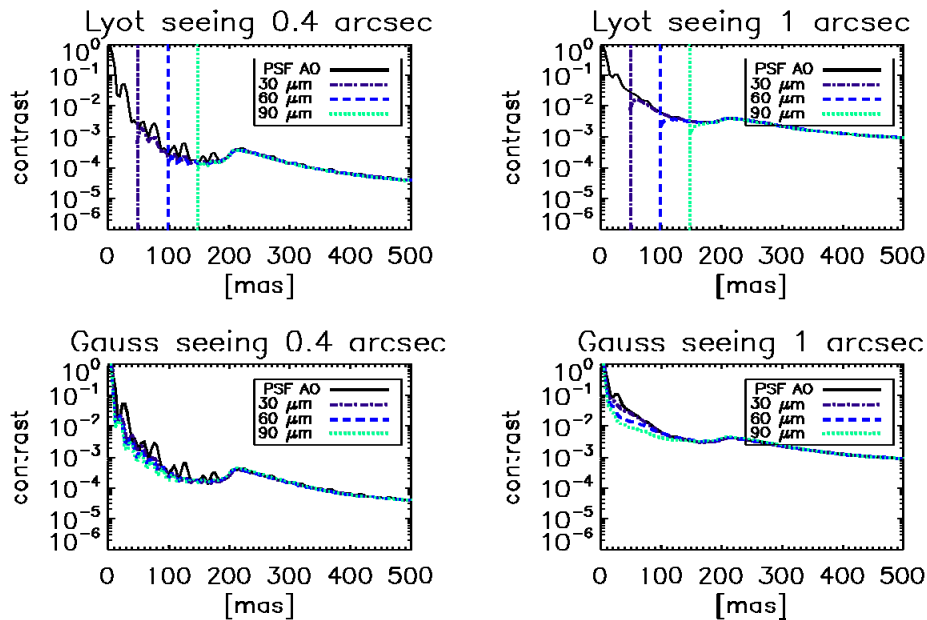
Figure 12. Left panels: contrast in R band for a Lyot with different radii and a Gauss mask with different HWHM. Right panels: as above but with different seeing conditions.

In Fig. 12 and Fig. 13 we show a comparative analysis of the performances of V-SHARK in R band in terms of contrast for 0.4 and 1 arcsec seeing conditions, and both Gauss and Lyot occulting mask of different sizes. More in particular, while in Fig. 2 the contrast is shown, in Figure 3 we plot the 10 σ detection curves for a magnitude 8 star. The vertical lines indicate the IWAs of each occulting mask in the legend. As expected, the contrast obtained is very sensitive to the seeing conditions with the contrast itself being of the order of 5 x 10⁻³ at 100 mas for 1 arcsec seeing, and 10⁻⁴ at 100 mas for 0.4 arcsec seeing. In contrast to this, the type of occulting mask used, as well as its dimensions, have a little effect on the final contrast curve, unless locations very close to the star are considered.

Please note that the contrast of the Gauss masks is multiplied by the transmission profiles, so that, on the contrary to the Lyot case, where the contrast is not definable within the IWA, it has a smooth trend towards the value of 1 when separation is approaching zero. However, it is worth noting that, when the detection curves are considered (see Figure

13), the Gauss occulter shows better performances with respect to the Lyot ones, at least when radial distances smaller than 200 mas are considered.

In order to study the 10 σ detectability as a function of the integration time, we considered a magnitude 8 star in R band, and a Lyot occulter (30 μm) with two different seeing conditions: 0.4 arcsec, and 1 arcsec. The results of this analysis for different integration times are shown in Fig. 14. The increase of contrast is at least one order of magnitude passing from 1 min to 60 min integration time. This holds for both seeing conditions, although for the 1 arcsec seeing the decrease of the contrast is significant (at least a factor of 10). It is worth stressing that the 10 σ represents a very demanding and safe detection constraint.
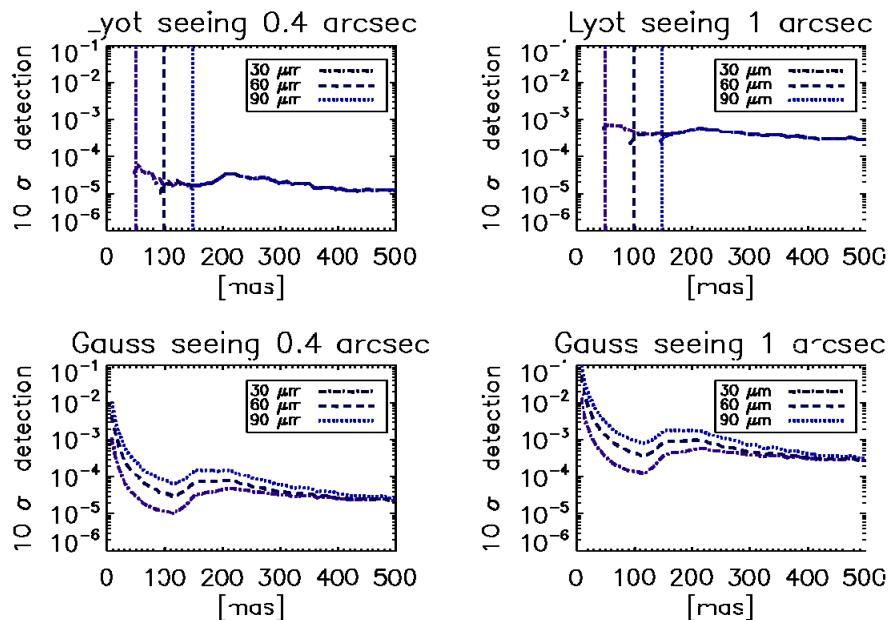


Figure 13: Left panels: detection curves in R band for a Lyot with different radii and a Gauss mask with different HWHM. Right panels: as above but with different seeing conditions.
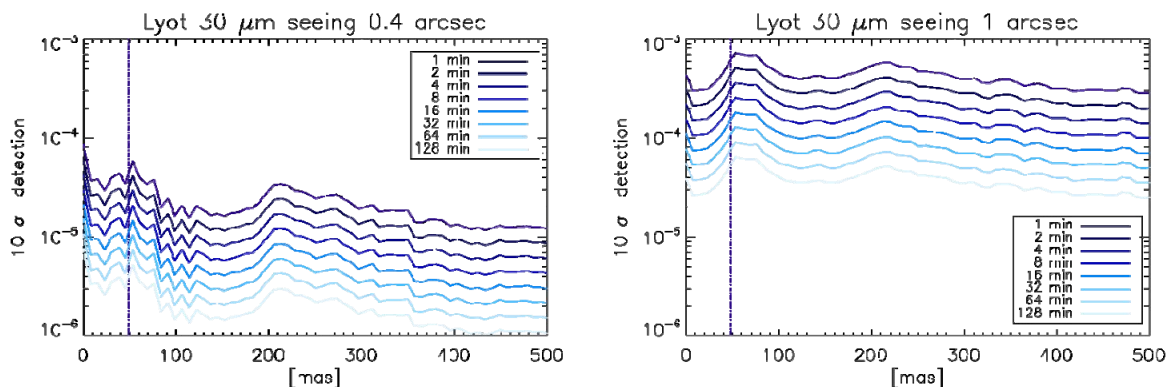


Figure 14: Detection curves, for a magnitude 8 star, in R band as a function of the integration time for seeing 0.4 arcsec (left) and 1 arcsec (right).

# 4. SCIENCE WITH V-SHARK

There are many science topics in which V-SHARK can give a unique contribution, both as a standalone instrument or coupled with its near-IR twin, SHARK-NIR [5], in following the typical LBT binocular philosophy. This features, coupled with its position in the northern hemisphere make V-SHARK a powerful competitor as well as a natural complement to the other two AO-fed instrument in the visual: SPHERE and GPI [11] [12].

A detailed list of science cases is being build up in these months by the science group, and some of the most interesting ones proposed up to now are shortly introduced in the following. Probably the most popular at present is the search for exoplanets, and in particular the direct detection of extra solar planets. Due to the very demanding resolution and contrast required on the scientific images, this is also a very challenging goal to achieve.

The competitivity of SHARK resides in its capability of reaching high Strehl ratio at moderately faint magnitudes (R > 10). An additional two magnitudes will be reached after the refurbishment of the AO system at LBT, opening the field of high-contrast AO imaging to stars much fainter than those feasible using the main SHARK competitors: SPHERE and GPI. The V-SHARK role is also important as a pathfinder to detect reflected light from giant planets, a topic where the instrument can be successfully used both in the visual and in the near infrared. While the NIR imaging can pick up the thermal contribution fo gas giant above 300 K, further contribution can come from imaging and IFU spectroscopy in the optical bands concerning albedo and spectral properties of the planets.

Other first grade science topics are listed below, with the specification of their visual-only or binocular potentialities:

- *disk around young stars and jets*: the study of protoplanetary disks is fundamental to comprehend he formation of our own solar system as well as of extra-solar planetary systems. This is a typical binocular case.

- *extragalactic science*: also in the extra-galactic field the unique capabilities of SHARK in terms of spatial resolution and contrast enhancement may be successfully applied: to study the feeding/feedback mechanism in nearby sources, the AGN-host relations as well as Dumped Ly-$\alpha$ systems (DLAs) and the quantum space-time degradation at high redshift.

- *high resolution/high contrast imaging*: detection and separation of close binaries, either in evolving systems or in degenerated system, in which one or both stars are in their final stages (white dwarfs, neutron stars, millisecond pulsar, high-mass X-ray binaries) are typical fields where to exploit the unique capabilities of V-SHARK

- *peculiar cases*: there are other science topics, somehow unusual, where V_SHARK can be tested with success: the quantum space-time degradation at high redshift, the measurements of the photon orbital angular momentum, and the use of lunar occultation to study RR Lyrae stars in binaries aiming at determining for the first time dynamical masses of RR Lyrae stars to improve the precision in determining the distance of stellar system hosting RR Lyrae stars.

# 5. V-SHARK TIMELINE

V-SHARK is planned as a fast track project with the aim to reach its first light, with the engineering software, in about 16-18 months after the FDR and to be full commissioned in the next 10-12 months with the final software. This requires an accurate and timely management of budget and resources.

The tentative Gantt chart of Figure 9 Right describes the project timeline, from the MOU signature for the CDP phase (June 17 2015), to the end of science verification. The most critical phases of installation at LBT and commissioning are zoomed in the left panel of the same figure, where several international travels are planned for the team members.

The development of the engineering software starts soon, after the CDP, and well in advance of the FDR to let the team enough time to layout an ICD with LBTO responsible about the high level control software and to verify the functionalities of the *drivers* for the selected hardware components. High level software development will start its prototyping just before the FDR.

Data reduction pipeline and ETC development start after the CDR to provide the commissioning team of V-SHARK with the right tools for data analysis and optimization of observation time during the science verification.
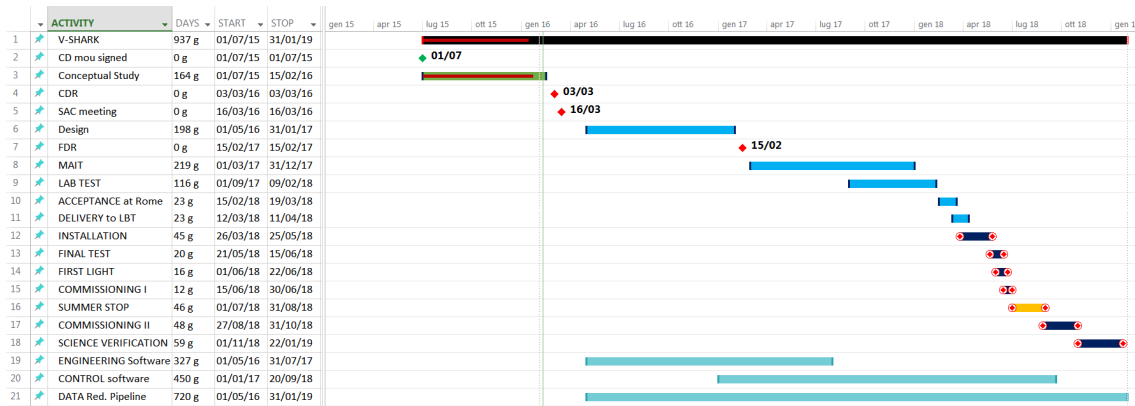
| # | ACTIVITY | DAYS | START | STOP |
|---|----------|------|-------|------|
| 1 | V-SHARK | 937 g | 01/07/15 | 31/01/19 |
| 2 | CD mou signed | 0 g | 01/07/15 | 01/07/15 |
| 3 | Conceptual Study | 164 g | 01/07/15 | 15/02/16 |
| 4 | CDR | 0 g | 03/03/16 | 03/03/16 |
| 5 | SAC meeting | 0 g | 16/03/16 | 16/03/16 |
| 6 | Design | 198 g | 01/05/16 | 31/01/17 |
| 7 | FDR | 0 g | 15/02/17 | 15/02/17 |
| 8 | MAIT | 219 g | 01/03/17 | 31/12/17 |
| 9 | LAB TEST | 116 g | 01/09/17 | 09/02/18 |
| 10 | ACCEPTANCE at Rome | 23 g | 15/02/18 | 19/03/18 |
| 11 | DELIVERY to LBT | 23 g | 12/03/18 | 11/04/18 |
| 12 | INSTALLATION | 45 g | 26/03/18 | 25/05/18 |
| 13 | FINAL TEST | 20 g | 21/05/18 | 15/06/18 |
| 14 | FIRST LIGHT | 16 g | 01/06/18 | 22/06/18 |
| 15 | COMMISSIONING I | 12 g | 15/06/18 | 30/06/18 |
| 16 | SUMMER STOP | 46 g | 01/07/18 | 31/08/18 |
| 17 | COMMISSIONING II | 48 g | 27/08/18 | 31/10/18 |
| 18 | SCIENCE VERIFICATION | 59 g | 01/11/18 | 22/01/19 |
| 19 | ENGINEERING Software | 327 g | 01/05/16 | 31/07/17 |
| 20 | CONTROL software | 450 g | 01/01/17 | 20/09/18 |
| 21 | DATA Red. Pipeline | 720 g | 01/05/16 | 31/01/19 |

Figure 9: V-SHARK preliminary Gantt diagram.

# 6. CONCLUSION

The V-SHARK team has evolved the original design of the SHARK visible channel towards a simple but efficient high resolution imager with the opportunity to offer also a coronagraph and an extension for an IFU spectroscope all of them working "diffraction limited" in the range of 600, 900nm with the assistance of AO. All the critical issues have been positively addressed and this project is now entering its final design review phase. The fast track of the project foresee its first light just 18 months after the FDR and it also will be well timed and synergic with the delivery of the NIR-SHARK and the future SOUL upgrade of the LBT AO system.

# ACKNOWLEDGMENTS

# REFERENCES

[1] Esposito, S., Riccardi, A., Fini, L., Puglisi, A. T., Pinna, E., Xompero, M., Briguglio, R., Quir´os-Pacheco, F., Stefanini, P., Guerra, J. C., et al., "First light ao (flao) system for lbt: final integration, acceptance test in europe, and preliminary on-sky commissioning results," in [SPIE Astronomical Telescopes+ Instrumentation], 773609–773609, International Society for Optics and Photonics (2010).

[2] Jefferies, S.; Hope, D.; Hart, M.; Nagy, J.: Proceedings of the Advanced Maui Optical and Space Surveillance Technologies Conference, held in Wailea, Maui, Hawaii, September 10-13, 2013, Ed.: S. Ryan, The Maui Economic Development Board, id.E52

[3] Pinna E. et al. SPIE 2016

[4] Pedichini et al. 2016 APJ submitted

[5] Farinato, J., Pedichini, F., Pinna, E., Baciotti, F., Baffa, C., Baruffolo, A., Bergomi, M., Bruno, P., Cappellaro, E., Carbonaro, L., Carlotti, A., Centrone, M., Close, L., Codona, J., Desidera, S., Dima, M., Esposito, S., Fantinel, D., Farisato, G., Fontana, A., Gaessler, W., Giallongo, E., Gratton, R., Greggio, D., Guerra, J. C., Guyon, O., Hinz, P., Leone, F., Lisi, F., Magrin, D., Marafatto, L., Munari, M., Pagano, I., Puglisi, A., Ragazzoni, R., Salasnich, B., Sani, E., Scuderi, S., Stangalini, M., Testa, V., Verinaud, C., and Viotto, V., "SHARK (System for coronagraphy with High order Adaptive optics from R to K band): a proposal for the

LBT 2nd generation instrumentation," in [Society of Photo-Optical Instrumentation Engineers (SPIE) Conference Series ], Society of Photo-Optical Instrumentation Engineers (SPIE) Conference Series 9147, 7 (Aug. 2014).

[6] Stangalini, M., Pedichini, F., Centrone, M., Esposito, S., Farinato, J., Giallongo, E., Quir´os-Pacheco, F., and Pinna, E., "The solar system at 10 parsec: exploiting the ExAO of LBT in the visual wavelengths," in [Society of Photo-Optical Instrumentation Engineers (SPIE) Conference Series ], Society of Photo-Optical Instrumentation Engineers (SPIE) Conference Series 9147, 8 (Aug. 2014).

[7] Farinato, J., Baffa, C., Baruffolo, A., Bergomi, M., Carbonaro, L., Carlotti, A., Centrone, M., Codona, J., Dima, M., Esposito, S., Fantinel, D., Farisato, G., Gaessler, W., Giallongo, E., Greggio, D., Hinz, P., Lisi, F., Magrin, D., Marafatto, L., Pedichini, F., Pinna, E., Puglisi, A., Ragazzoni, R., Salasnich, B., Stangalini, M., Verinaud, C., and Viotto, V., "The NIR arm of SHARK: System for coronagraphy with High-order Adaptive optics from R to K bands," International Journal of Astrobiology 14, 365–373 (July 2015).

[8] A. Ghedina & R. Ragazzoni (1997) Optimum configurations for two offaxis parabolae used to make an optical relay, Journal of Modern Optics, 44:7, 1259-1267

[9] Bailey, V. P., Hinz, P. M., Puglisi, A. T., et al. 2014, in Proc. SPIE, Vol. 9148, Adaptive Optics Systems IV, 914803

[10] Krist, J. E., "PROPER: an optical propagation library for IDL," Optical Modeling and Performance Predictions III (2007).

[11] Jean-Luc Beuzit ; Markus Feldt ; Kjetil Dohlen ; David Mouillet ; Pascal Puget, et al. "SPHERE: a 'Planet Finder' instrument for the VLT", Proc. SPIE 7014, Ground-based and Airborne Instrumentation for Astronomy II, 701418 (July 08, 2008)

[12] Macintosh, B. A., Graham, J. R., Palmer, D. W.,et al. 2008, in Proc. SPIE, Vol. 7015, Adaptive Optics Systems, 701518

[**] The SHARK science team:

F. Ambrosino[2], S. Antoniucci[2], F. Bacciotti[3], C. Baffa[3], S. Benatti[1], M. Bergomi[1],M. Bonavita[1], A. Bongiorno[2], L. Borsato[8], E. Brocato[2], P. Bruno[4], E. Cappellaro[1], L. Carbonaro[3], A. Carlotti[5], M. Centrone[2], R. Claudi[1], L. Close[6], J. Codona[6], F. Cusano[13], S. Desidera[1], M. Dima[1], V. D'Orazi[1], S. Esposito[3], J. Farinato[1], G. Farisato[1], F. Fiore[2], A. Fontana[2], W. Gaessler[7], E. Giallongo[2], T. Giannini[2], V. Granata[8], D. Greggio[1], J.C. Guerra[6], T. Henning[7], J. Hill[12], P. Hinz[6], R. Gratton[1], D. Kopon[7], F. Leone[9], G. Li Causi[2], F. Lisi[3], D. Lorenzetti[2], D. Magrin[1], A.-L. Maire[1], C. Maceroni[2], L. Malavolta[8], L. Marafatto[1], F. Massi[3], D. Mesa[1], G. Micela[11], G. Molina Terriza[15], M. Munari[4], V. Nascimbeni[8], R. Neo[15], B. Nisini[2], I. Pagano[4], F. Pedichini[2], E. Pinna[3], G. Piotto[8], L. Podio[3], R. Ragazzoni[1], A. Richihi[14], L. Sabatini[2], E. Sani[3], G. Scandariato[4], S. Scuderi[4], E. Sissa[1], A. Sozzetti[10], M. Stangalini[2], V. Testa[2], M. Turatto[1], C. Veillet[12], C. Verinaud[5], V. Viotto[1], S. Zibetti[3], A. Zurlo[1]

Affiliations of the V-SHARK Science Team:

1) INAF Padova; 2) INAF-OAR Monte Porzio; 3) INAF-Arcetri; 4) INAF-Catania; 5) IPAG; 6) Steward Observatory; 7) MPIA; 8) University of Padova; 9) University of Catania; 10) INAF-Torino; 11) INAF-Palermo; 12) LBTO; 13) INAF-Bologna; 14) NARIT Thailand; 15) University of Sydney